Schottky-barrier formation at nanoscale metal-oxide interfaces

D. L. Carroll
Department of Materials Science and Engineering, University of Pennsylvania, Philadelphia, Pennsylvania 19104-6272

M. Wagner and M. Rühle
Max-Planck-Institut für Metallforschung, Institut für Werkstoffwissenschaft, D-70125 Stuttgart, Germany

D. A. Bonnell
Department of Materials Science and Engineering, University of Pennsylvania, Philadelphia, Pennsylvania 19104-6272

(Received 26 July 1996)

Isolated, nanoscale (5.0–20.0 nm diameter) Cu clusters on a reduced TiO_2 (110) surface exhibit the initiation of the Schottky effect. Apparent height changes of isolated clusters occur in scanning tunneling microscopy imaging as bias conditions are changed. This apparent height change is directly related to current flow through the cluster-oxide interface barrier. Further, depletion zones along the substrate surface adjacent to the clusters exhibit the same bias dependence indicating that changes are associated with local band-bending, analogous to that of macroscopic Schottky barriers. Barrier-height variations with cluster size and with applied voltage are quantified. When compared to models of edge effects in finite-sized systems a direct correlation between geometry and barrier formation is made. [S0163-1829(97)05511-2]

INTRODUCTION

The properties of metal-semiconductor interfaces have been a major theme of solid-state physics for many years. The relevance to device development in both high-speed computing and electronics applications, as well as in opto-electronics, has made a quantitative understanding of interface electronic structure imperative. Presently, device integration technology requires uniform device performance at the length scales below 1 μm. At these sizes, substrate imperfections can yield wide variation in interface, junction, and depletion zone characteristics.

One macroscopic characteristic of a metal-semiconductor interface is the formation of a Schottky barrier (SB) and the related depletion zone extending into the semiconductor. Though a complete understanding of SB formation has been elusive, it is well known that even on continuous, thick films, there is a wide variation in barrier heights at the interface. Several comprehensive studies on Schottky-barrier height (SBH) variations at nonideal interfaces exist, but few address phenomena on the nanometer size scale. Sullivan employed numerical simulations and TEM to characterize inhomogeneities at interfaces.[1,2] Submicrometer patches with low SBH's embedded in a continuous film of high SBH were shown to have been averaged in the macroscopic measurements. Tung has summarized the effects of nanometer scale irregularities with specific geometries concluding that a detailed knowledge of the potential near edges is necessary to understand size effects.[3–5] Several groups have applied ballistic-electron-emission microscopy (BEEM) to the study of SBH inhomogeneities. Palm, Arbes, and Schulz have shown that randomly distributed defects at the interface appear as areas of low-effective SBH in BEEM images.[6] Hecht *et al.* have shown BEEM images of Au/GaAs (100) with nanometer-sized domains with SBH variations of more than 0.04 eV.[7] Finally, Stiles and Hâmann theoretically addressed the problem of different interface structures in SBH measurements made with BEEM. However, these results must be interpreted in the limit of infinite, continuous contacts.[8] Thus, nanometer-scale spatial variations in SB formation are ubiquitous but not yet well understood.

One approach to addressing this issue is to produce nanometer-scale metal-semiconductor contacts and make local determinations of contact potentials. The copper metallization of TiO_2 (110) presents an interesting case in Schottky-barrier formation because a wide degree of variability in surface stoichiometry can be accommodated by the transition-metal oxide. Full interfacial-barrier formation on materials with wide band gaps (3.0 eV in this case) can require significant band bending and field penetration into the substrate. While initial studies of Cu film growth on TiO_2 (110) suggested Stranski-Krastanov growth,[9,10] there now is convincing evidence that the film growth of Cu on TiO_2 is Volmer-Weber-like, indicating a small interaction between metal overlayer and the substrate and the potential for the formation of small metal clusters. This system has been studied using a variety of surface analytical probes. Diebold, Pan, and Madey[11] have shown that Volmer-Weber growth occurs at low coverages using secondary ion-mass spectroscopy and x-ray photoemission spectroscopy. Thibado and Bonnell[12,13] applied scanning tunneling microscopy (STM) to Cu films grown on TiO_2 (100) showing the existence of clusters, as did Novak.[14]

In this work, the formation of interface barriers between nanometer Cu clusters and TiO_2 (110) are examined to determine the factors contributing to their development. The tunneling behavior and local surface structures of TiO_2 (110) are among the better understood of transition-metal oxides.[15–17] Voltage-dependent STM imaging of TiO_2 has not been reported and is indeed rare in transition-metal oxides. In the present work, the voltage-dependent contrast of isolated copper clusters is quantified and related to the elec-

0163-1829/97/55(15)/9792(8)/$10.00 © 1997 The American Physical Society

tronic properties of the interface between the copper and the oxide. Changes in the apparent height of the clusters at different biases are shown to be related to changes in the local conductivity through the cluster-oxide interface. This conductivity is, in turn, related to the bias of the interface relative to the contact potential, due to band bending at the interface. We find the contact potential to be size dependent, not reaching the macroscopic Schottky value until the cluster diameter exceeds 25 nm. Further, a simple model for barrier formation which is dominated by edge effects at these size scales is proposed.

EXPERIMENTAL PROCEDURES

The surface stoichiometry, electronic structure, and atomic structure of transition-metal oxides are extremely sensitive to processing and thermal history. The reproducible preparation of stepped, ordered surfaces requires careful quantification. A method of producing a surface which, when imaged by STM, shows steps of approximately 0.33 nm and atomically flat terraces was developed.

Preparation of TiO_2 (110)

Standard analysis, sample preparation, and metal deposition were carried out in an ultrahigh vacuum (UHV) system with a typical base pressure of 5×10^{-10} torr. Residual gas analysis (Anavac) of the UHV system showed that the primary composition of the background gas was H_2, with trace amounts of H_2O. Partial pressures of all other gases were below 1×10^{-11} torr and were considered insignificant for the time scale of these experiments. During operation of the Knudsen deposition cell, vacuum pressure rose to the 10^{-9}-torr range with a small increase in the H_2 and H_2O partial pressures detected. Generally, the metal source was operated only when the substrate was at temperatures above 300 °C, further reducing the likelihood of surface contamination.

The substrate was cut from a single-crystal boule of Nb-doped TiO_2. The dopant level was 0.01% by weight to allow sufficient conductivity for tunneling and the crystal appears deep blue. With substantial bulk reduction, the crystal becomes gray. Orientation to within 0.5° of the (110) surface was verified using Laue diffraction. The surface was polished with a 0.03 μm grit and ultrasonically cleaned in acetone and methanol. All heating was done with an e^- beam heater from the back of the sample so that no electron-stimulated desorption would occur from the face that was to be imaged. The surface temperature was measured using two K-type thermocouples placed on either side of the sample and calibrated with optical pyrometry. A short sputter and anneal cycle was carried out to clean the surface. When imaged with STM this surface exhibited no steps or atomic scale features. After several cycles of 500 eV Ar^+-ion sputtering (between 15 and 60 min) and annealing at 600 °C (between 15 and 60 min) a flat surface with 0.33 nm steps could be obtained reproducibly. The method for producing this surface is similar to that used by other researchers.[18] This procedure was carried out on four different substrates cut from the same boule. In every instance, STM images revealed a stepped surface structure. Core-level and valence-band x-ray photoemission spectroscopy showed that the degree of reduction at the surface was below the detection limits of the XPS spectrometer. There were no traces of Ti^{3+} or Ti^{2+} in the spectra and emission from gap states was within the noise.

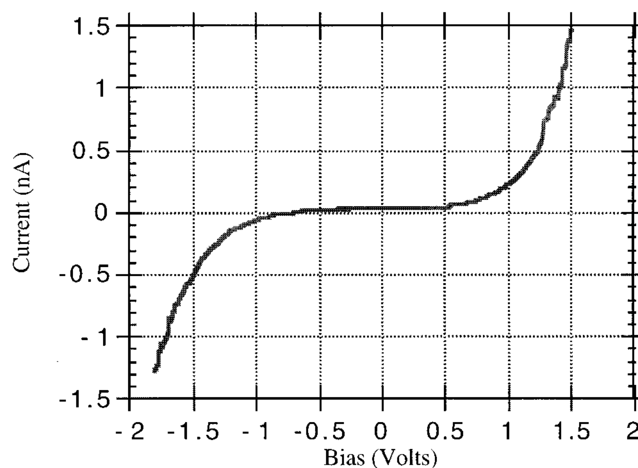

FIG. 1. Tunneling spectrum acquired at a setpoint of −1.5 V and 0.5 nA, on a flat terrace away from deposited metal or step edges.

STM images were acquired in constant-current mode using a commercially available instrument (Park Scientific). Typical imaging setpoints were 1.5–3.0 V with a current of 0.5 nA. In all cases, the surfaces were imaged with mechanically formed Pt-Ir tips. Tunneling-spectroscopy measurements acquired on the terraces of these surfaces showed a slight rectification as seen in Fig. 1. The tunneling spectra on stepped surfaces were generally distinguishable from those taken on heavily reduced (annealed above 800 °C for 60 min without sputtering) both in Fermi-level position and in shape.

In an effort to quantify the effect of H_2 adsorption from the background gas, the stepped surface was imaged over a 6-h period, during which the vacuum composition was monitored. Under the conditions of our system, the surface of clean TiO_2 (110) exhibits significant contamination (likely H_2 adsorption) after 4 h exposure to the vacuum at room temperature. This contamination appears as indistinct cloudlike features decorating the step edges initially and covering the step in time. The diameter of the cloudlike features was approximately 1.0 nm. The surface could then be cleaned by flash heating to 500 °C for a few seconds and the images return to the stepped structure described above.

Cu deposition

Copper was deposited onto the surface under a variety of conditions, using a custom-built Knudsen cell with 99.98% purity copper and tungsten heating filaments. The source-to-sample distance was approximately 5.0 cm. Coverage was estimated by measuring the temperature (using thermocouples and optical pyrometry) of the cell and using published sublimation rates to estimate the flux. The cell was aligned such that the incident-mass flux was parallel to the surface normal, ensuring a relatively homogeneous deposition across the surface. Uncertainty in the metal coverage is estimated to be 0.5 ML. Cell conditions were constant for

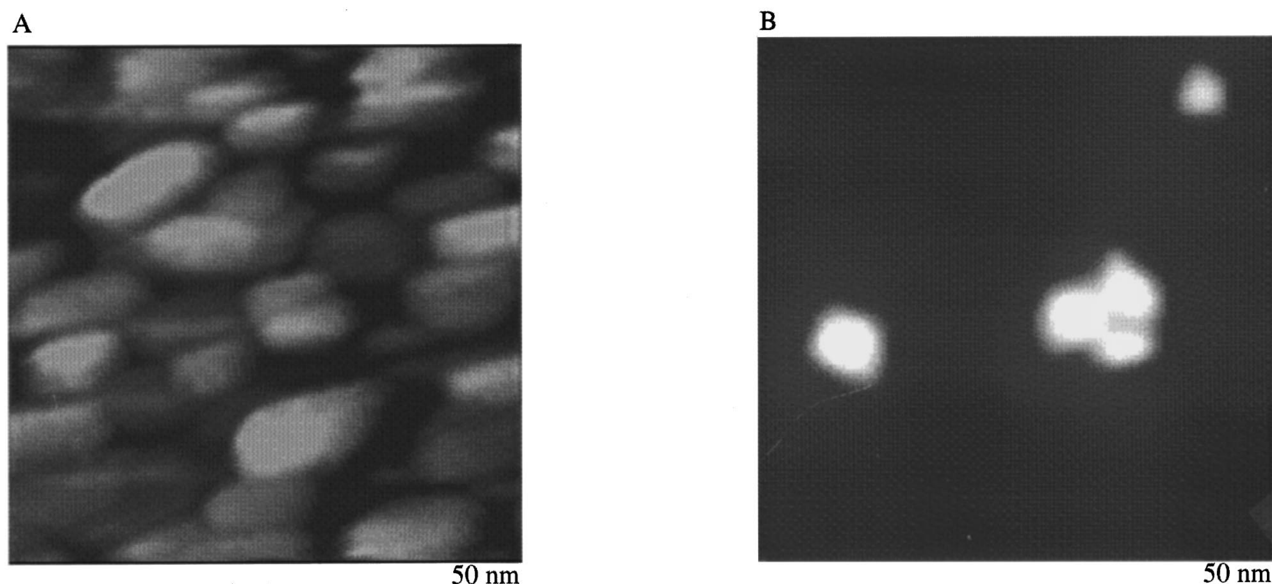

FIG. 2. Constant-current images of the surface after a 2-ML deposition of Cu at a substrate temperature of 300 °C acquired at −1.5 V and 0.5 nA. (a) 50×50 nm^2 area of an agglomerated region with the black to white scale 5.0 nm. (b) 50×50 nm^2 area acquired over an area of low-mass density with a black to white scale of 2.3 nm. Note the difference in cluster size and distribution homogeneity.

each deposition; therefore error in the metal coverage estimate is expected to be systematic.

The deposition of 1–2 ML of Cu onto oxide surfaces such as TiO_2 (110) at room temperature is known to result in three-dimensional clusters.[11] Figure 2(a) shows a 50×50 nm^2 image of the close-packed regions. Cluster diameters range from 10 to 20 nm with heights of approximately 5 nm. Similar to results of copper deposition on $SrTiO_3$,[19] most of the copper clusters appear to have aggregated into domains of randomly close-packed clusters while others seem pinned in areas with low-cluster density. Thus, on these length scales, the morphology is clearly inhomogeneous. Figure 2(b) shows a 50×50 nm^2 region of low-metal density that is immediately adjacent to the edge of the agglomerated domain. Clusters of approximately 5–20 nm [Fig. 2b shows only the smaller clusters] occur in a random distribution over the terrace. It is important to note, however, that some clusters in the regions of low mass density are sometimes quite mobile while others seem pinned to the surface.

RESULTS AND DISCUSSION

Images of areas with high cluster density, in which the clusters have agglomerated, exhibit little dependence on the polarity of the tip bias used to acquire the image; however, where the clusters are clearly isolated and distinguishable from each other, there is a strong polarity dependence in the measured size of the cluster.

Bias dependence in nanostructure morphology

The effect of sample-tip bias on apparent cluster size is shown in Fig. 3. A comparison of the same cluster acquired at two different samples-to-tip biases is shown in cross section, by scanning the same line twice and alternating the polarity between each scan. While the magnitude of the tunneling current is constant, line scan A was acquired with the current flowing into the sample at a bias of 1.5 V, while for line scan *B*, the current was reversed with a bias of −1.5 V. Note the change in apparent height (contrast with respect to the background plane). This effect was observed on all images of isolated clusters; however, it was not observed on the agglomerated region.

To quantify the effects of voltage on the morphology of the isolated clusters, the surface plane was identified by the pixel average over an area without steps. This plane was then used for reference in cross-sectional analysis of the clusters. Randomly chosen cross sections through the cluster center were extracted from the image and the maximum heights with respect to the surface plane determined. In each case,

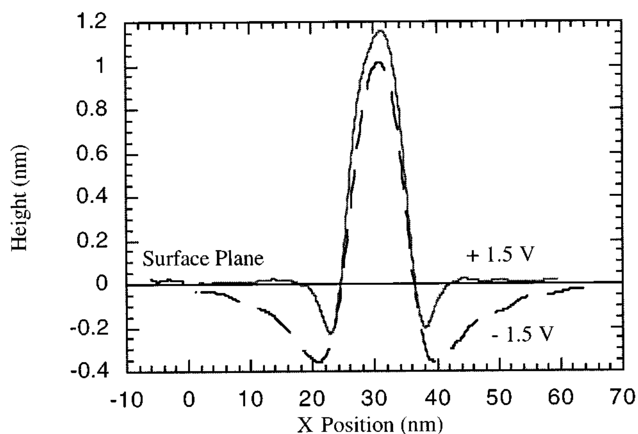

FIG. 3. Line scans of a single-isolated cluster acquired at two different bias voltages with the feedback used in constant-current mode. Solid line was acquired at 1.5 V and 0.5 nA. The current flow is from tip into sample. Long-dashed line was acquired at −1.5 V and 0.5 nA. The current flow is from sample into tip. Zero height represents the location of the ''real'' surface, determined by pixel average. A depression on either side of the cluster is observed in all the data.

the values reported are the average of at least ten measurements. Cluster diameter was determined in a similar manner, using the intersection of the extracted-cluster profile with the surface plane as the location of the "physical interface." The estimated measurement error in the height measurement was 0.01 nm and in the diameter measurement was 0.1 nm. Of the roughly 30 clusters discussed here, three changed their overall shape and position during the measurements. In these instances, though no evidence of "tip change" was observed, it is assumed that the clusters were sufficiently mobile to be affected by the tip and were ignored. Consequently, it may be that our study is weighted toward clusters with strong interface interactions.

Tip-displacement effects

Several factors can lead to an apparent height change with sample-tip bias in STM images. The difference in applied bias implies a variation in the set-point conditions for tunneling. This effect can have two consequences: electronic effects imposing a change in sample-tip separation and geometric effects resulting from resolution loss due to an increased imaging height. The magnitude of these effects in observed contrast can be estimated using the tunneling spectrum taken on the TiO_2 (110) terraces and are discussed below.

The change in height from the TiO_2 plane imposed by the difference in the density of states at given tunneling voltages, is approximated by applying the tunneling equation:

$$I \sim V\rho_s(0,E)\exp[-1.025\phi^{1/2}W] \tag{1}$$

which relates the tunneling voltage (V, the voltage applied between the tip and the sample), density of states of the surface evaluated at the tip for the electron energy E $[\rho_s(0,E)]$, tunneling barrier (ϕ), and the tunneling-gap width (W).[20] Using 0.5 nm as an initial guess at the tunnel-gap width, 5.65 eV for the work function of Pt,[21] 4.8 eV for the electron affinity of $TiO_2(\chi)$,[22] a trapezoidal approximation to the vacuum-barrier shape, and the values ± 1.5 V and $-1.3/+0.5$ nA from Fig. 1, relative values for $\rho_s(0,E)$ can be found. This can be carried out for each voltage to estimate the change in W due to the change in $\rho_s(0,\mathrm{E})$ as seen in the tunneling spectra. Thus we get $\Delta W = 0.02 \pm 0.01$ nm, which represents the total change in the tunneling-gap width over the TiO_2 planes when the tunneling voltage is shifted from $+1.5$ to -1.5 V. This approach cannot be used to estimate changes while the tip is over the metal cluster because the tunneling gap will be affected by the cluster-oxide interfacial barrier. However, inverse photoemission and photoemission show that the density of filled and unfilled states is the same at $+1.5$ and -1.5 V.[23] Therefore, the change in tunneling conditions (i.e., the change in tunneling voltage from $+1.5$ to -1.5 V) over copper results in little, if any, change in tip position due to the bulk-band structure of the copper. This effect, due to purely electronic-structural differences in the substrate at the different voltages, is shown schematically in Fig. 4. Since the distance that the tip must move in z as it travels from surface to metal changes, the apparent height of the cluster must change by 0.02 ± 0.01 nm.

The geometric effect of changing sample-tip separation must also be taken into account since it results in a change in the observed corrugation amplitude of surface features. The observed corrugation-amplitude change according to Stoll *et al.*[24] is given by the expression:

$$\Delta/\Delta_0 = \exp\{-\pi^2/a^2(R+W)/\kappa\}, \tag{2}$$

where $2\pi/a$ is the reciprocal lattice vector of longest Fourier component, R is the tip radius (2.5 nm), W is the tunneling-gap width from the TiO_2 surface, $\kappa^2 = (2m\phi)/h^2$, m is the electron mass, h is Planck's constant divided by 2π. Reasoning that the formula of Stoll *et al.* can be applied to the longest Fourier component of the features of interest and assuming a Fourier component the size of the cluster gives an estimate of total change in apparent height as $\Delta W_{\mathrm{total}} = 0.03 \pm 0.01$ nm. Underestimating the tip radius yields a conservative estimate of the effect; if the tip size is larger, the effect is even smaller. Therefore, the maximum change in the measured height of a given cluster, due to both the electronic and geometric consequences of the difference in tunneling conditions (at voltage shifts of around 3.0 V), is of the order of 0.05 nm. Any change larger than this must be attributed to other factors.

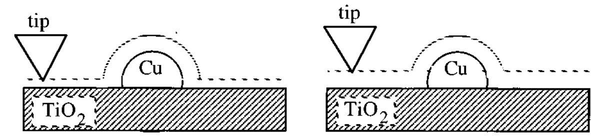

FIG. 4. A schematic diagram of the relative sample-tip separation on the TiO_2 and over the metal cluster. The effects of a change in setpoint are illustrated by the dashed line.

Apparent cluster size

The observed cluster-height changes supersede the above estimate by nearly an order of magnitude and are strongly dependent on the total voltage variation in the two images. Figure 5 shows the dependence of apparent height change on voltage (ΔV) for a cluster diameter of 13.0 nm. Clearly, the effect of the contact between the cluster and the substrate must be taken into account. The configuration is schematically illustrated in Fig. 6 which labels the relationships between the energies of the tip, Cu cluster, and semiconducting

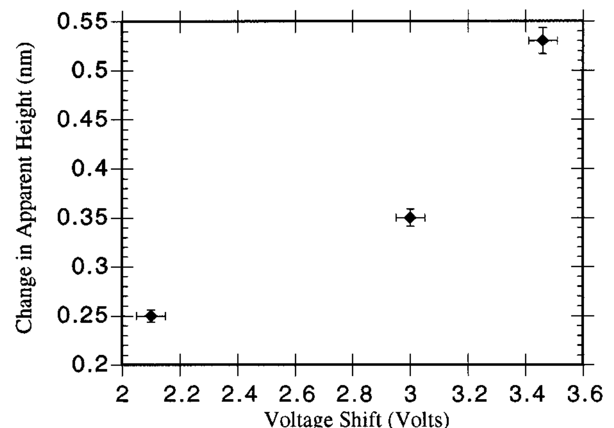

FIG. 5. The apparent change in height as a function of total-voltage change.

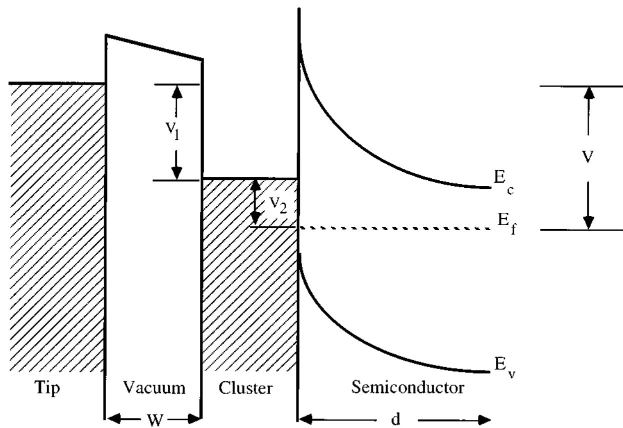

FIG. 6. Band-level diagram of cluster imaging as a two-step tunneling process. The diagram shows the condition in which electrons flow from the tip into the sample, or reverse bias of the interface.

substrate electrons when the tip bias is negative with respect to the cluster-substrate system. The doped TiO_2 is an n-type semiconductor; therefore ideally, with no external bias, the interface potential is $\phi_{\mathrm{copper}}-\chi_{\mathrm{rutile}}=0.85$ V, in the Schottky limit.[25] As shown in Fig. 6, when the system is biased, the Fermi levels are offset by V_1 at the tunnel junction and V_2 at the interface, since a measurable current in the STM implies transport through the vacuum barrier (W) and across the depletion region of the substrate (d). When the interface is biased, the resulting band bending gives an ''effective barrier'' to current flow that is voltage dependent. Thus, tunneling out of the substrate, out of the cluster, and into the tip (forward bias) results in an interfacial barrier which is smaller than the contact potential. A reverse bias, tunneling into the cluster and into the substrate, increases this effective barrier slightly and reduces the interface transmission probability. The effective interfacial barrier to current flow is voltage dependent. The contact potential at the interface is a material parameter and is not voltage dependent; though, as we will show later, this contact potential is not fully a Schottky barrier in the classical sense, we draw the analogy in a manner similar to the references cited above (i.e., the onset of Schottky contact behavior).[26] The tip moves away from the surface of the cluster in the forward-bias condition and toward the cluster surface in the reverse-bias condition to maintain a constant tunneling current as measured by the STM feedback system. The apparent height changes of the clusters with bias correspond to differences in the copper-substrate interfacial-depletion region under the forward- and reverse-bias conditions. Further, as in any Schottky diode, it is expected that an increase in the magnitude of bias change would increase the total amount of band bending and, consequently, the total change in effective barrier between the two voltages. This is observed in that the apparent contrast change of the cluster increases with the size of the voltage swing. This is equivalent to saying that the total voltage drop over the cluster-substrate system (V_1+V_2) is the applied voltage of the STM (V) and that the total tunneling gap is the sample-tip separation plus the depletion zone ($W+d$) (see Fig. 6). When the voltage is shifted from $+1.5$ to -1.5 V the value of $W+d$ must remain constant except for the minor adjustment due to differences in band structure discussed above. Thus, if d is increased, W must decrease and vice versa. The change in W is measured as a change in apparent height of the cluster.

In addition to an apparent cluster height change, the contour of the surface near the cluster is voltage dependent. The apparent depression is the response expected in a region depleted of carriers as would be the consequence of a localized interfacial barrier. The barrier height at the interface can be estimated by measuring the lateral depletion zones near the cluster. Again referring to Fig. 3, these cross sections of the 15.0 nm cluster show depressions adjacent to the cluster edges. Recall, the line scans were acquired at sample biases of (+) -1.5 V; therefore the interface is (reverse) forward biased. The fact that the size of this apparent depression is a function of voltage indicates that it is an electronic effect rather than a topographic feature and results from a capacitive coupling between cluster and tip. The contour of this region lies below that of the plane far from the cluster. If the shape of the contour on the surface is assumed to be that of the depletion zone, the contour can be fit and integrated to find the volume. Using the ''abrupt-junction approximation''[26,27] and a majority carrier density of $10^{18}/\mathrm{cm}^3$ (specified by the crystal-dopant concentration), the forward-biased interface barrier effective height is 2.2 mV and the reversed-biased barrier effective height is 22.0 mV. Again, as stated above, the effective height of the interface barrier in this case refers to a barrier to current flow based on the width of the depletion zone under bias. It can be related to the contact potential through some choice of transport model. In macroscopic systems, this value is typically associated with the Schottky barrier height minus the applied bias at the interface ($\Phi_{\mathrm{effective}}=\Phi_{\mathrm{Schottky}}-V_2$). However, since the effective barrier heights above are given for the forward- and reverse-bias conditions of the contact, the contact potential associated with the interface lies somewhere between these values.[26]

Apparent height changes and lateral depletion regions are also strongly dependent on the cluster diameter, as shown in Fig. 7. The smallest particles exhibit apparent height changes of nearly 0.2 nm, larger than that predicted to result from changes in sample-tip separation as discussed above. The general trend of this dependence was observed when the total voltage shift was ±1.0, ±1.5 (as shown), and ±1.8 V.

Edge effects

Edge effects have been characterized in SB inhomogeneities for some geometries, including strips and circular patches of low SBH interfaces imbedded in an interface of high SBH.[1] Though this is exactly the inverse of the system under study, the same physical intuition may be applied. Again, in this study, the analogy to the classical Schottky barrier is made. For simplicity, the term ''effective barrier'' is used to describe the barrier to current flow at the metal-semiconductor interface and is distinct from the contact potential. In the present case, the electric-field density beneath the cluster varies laterally across the interface. Near discontinuities of the interface, the field density should be large due to the edge of the metal film. At the center of the cluster, the field density should be similar to that of an infinite plane of charge.[28] Therefore, band bending near the edge of the clus-

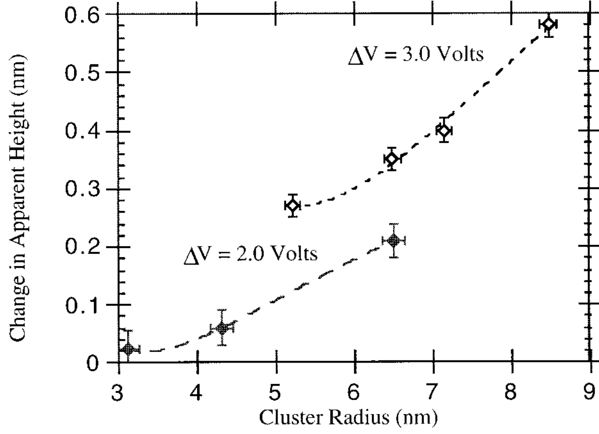

FIG. 7. Apparent height change as a function of cluster diameter. The four points shown for $\Delta V = 3.0$ V, represent ten data points with several points overlapping. The three from the $\Delta V = 2.0$ V, represent eight different data points with some points overlapping. These data were collected for heights measured at 1.5 and -1.5 V and a tunneling current of 0.5 nA. Similar functional dependences are seen for a voltage shift from 1.0 to -1.0 V.

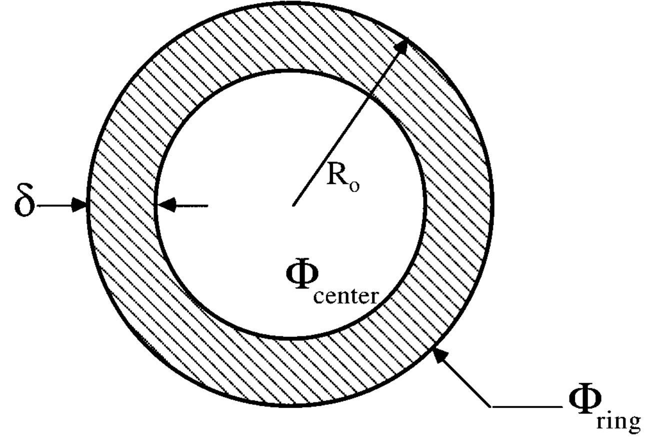

FIG. 8. A schematic representation of the model for edge effects in the measured barrier height. The cluster area in contact with the substrate is divided into two regions; a ring of low-contact potential and a central area of higher-contact potential. The low potential is due to edge effects in the field near the edge of the cluster.

ter should be greater. Because the Fermi level of the cluster and the electron affinity of the semiconductor are fixed relative to each other across the interface, more current will flow through the edges of the structure. This situation is similar to that of ''leakage'' currents in ultra-large-scale integration capacitors.[27] To estimate its effects in STM imaging of nanoscale contacts, we note that the field density, and thus the contact potential at the interface must vary smoothly. The interface is partitioned into two separate regions, an area of low-contact potential associated with the edge of a cluster, $\Phi_{\rm ring}$, and an area of high-contact with the center of the cluster, $\Phi_{\rm center}$. In contrast to the above-mentioned situation, the effective low barrier height derives from the finite size and is taken to be the mean value of the smoothly varying function of the barrier height at the edge.[4,29] The contact potential in the center of the cluster is that associated with Schottky-barrier development in an infinite, continuous film of copper on TiO_2 (110) (i.e., $\phi - \chi$). Assumed implicitly is that the cluster behaves as a metal and when unbiased, the Fermi levels of the cluster and the substrate match. The relative contributions of the two different areas in the overall current flow through the region is the sum of the current flow through a small annulus around the edge of the cluster and that through the center of the cluster as shown in Fig. 8. The relative magnitudes of the contact potentials are $\Phi_{\rm center} > \Phi_{\rm ring}$, $\Phi_{\rm center} = {\rm const}$ for $0 < r < R - \delta$, and $\Phi_{\rm ring} = {\rm const}$ for $R - \delta < r < R$, where R is the radius of the contact area, and δ is the part of the radius associated with the annulus. This is equivalent to saying that the manifestation of the lower contact potential at the edge will be a smaller depletion region and thus a higher current density across that part of the contact. The effective depletion regions associated with these contacts are taken to have the same geometric dependence as does the potential-barrier distribution, that is, distinct depletion depths are associated with the center and the annulus regions. Since this does not take into account the complexities of the potential at the edge of the cluster, it seems reasonable to expect that any error in the approximation should be associated with the value chosen for δ. The interest here is how the area of the annulus in which the edge-related effects occur, contributes to current flow through the interface as a function of cluster diameter. Expressing the ratios of partitioned areas to the total area in terms of the above variables:

$$\frac{A_{\rm ring}}{A_{\rm total}} = \frac{2\delta}{R} - \frac{\delta^2}{R^2},$$

$$\frac{A_{\rm center}}{A_{\rm total}} = 1 - \frac{2\delta}{R} + \frac{\delta^2}{R^2}. \tag{3}$$

When R becomes large, the proportion of the ring area to the total area becomes vanishingly small and the area of the center dominates, as expected. Assuming that the currents through all partitions of the cluster-semiconductor interface must add to equal the total current through the vacuum gap of the STM, an upper bound on the edge effect as a function of cluster radius can be derived. The current through the system, by charge conservation, is therefore related by

$$[A_{\rm ring} J_{\rm ring} + A_{\rm center} J_{\rm center}] = V \rho_s(0,E) \exp[-1.025 \phi^{1/2} W], \tag{4}$$

where J (V_2, contact potential, $T = 25$ °C) is the current density, V is the voltage applied between the sample and tip, V_1 is the voltage dropped across the vacuum barrier, V_2 is the voltage dropped across the cluster-semiconductor interface, A_i is the area of respective partitions of the interface, ϕ is the average work function of the Cu cluster and the Pt-Ir tip $= 5.0$ eV, and $\rho_s(0,E)$ is the density of states at energy $2eV_1$ evaluated at the tip center. Implicit in this expression is the assumption that no ballistic transport takes place through the cluster and into the semiconductor. This assumption is made because the magnitude of the current is much larger than that of typical BEEM experiments, in which ballistic transport is

the primary mechanism. Figure 6 shows the relation between these parameters and the total voltage applied by the STM. Rearranging terms:

$$W=\frac{\ln\{[A_{\text{ring}}J_{\text{ring}}+A_{\text{center}}J_{\text{center}}]V^{-1}\rho^{-1}\}}{1.025\phi^{1/2}}. \tag{5}$$

The negative sign is lost by taking the sense of the voltage and the current to be positive. In this experiment, variations in the apparent height (vacuum gap width) with voltage are the measured quantities. Writing the height difference in terms of local conductivities, while $G_i=J_1/V$:

$$\frac{dW}{dV}=\frac{1}{1.025\phi^{1/2}}\left[\frac{G'_{\text{ring}}A_{\text{ring}}}{G_{\text{ring}}A_{\text{ring}}+G_{\text{center}}A_{\text{center}}}+\frac{G'_{\text{center}}A_{\text{center}}}{G_{\text{ring}}A_{\text{ring}}+G_{\text{center}}A_{\text{center}}}\right]. \tag{6}$$

The derivative G'_i is taken with respect to the sample-tip applied voltage. The conductivities are assumed to be functions of the applied voltage through dependences on V_1 and V_2. No specific form has been specified for the current densities though, the standard equations for current flow through a potential barrier would be a good first approximation. To emphasize the geometric dependence, the denominators are written in terms of effective properties and Eq. (1) is substituted for the areas:

$$\frac{dW}{dV}=\frac{G'_{\text{ring}}A_{\text{ring}}}{G_{\text{eff}}A_{\text{total}}}+\frac{G'_{\text{center}}A_{\text{center}}}{G_{\text{eff}}A_{\text{total}}}=\frac{G'_{\text{center}}}{G_{\text{eff}}}+\frac{2\delta(G'_{\text{ring}}-G'_{\text{center}})}{RG_{\text{eff}}}+\frac{\delta^2(G'_{\text{center}}-G'_{\text{ring}})}{R^2G_{\text{eff}}}. \tag{7}$$

Note that the first and third terms are positive while the second is negative. This picture yields the intuitive result that the variation in the tunneling gap (between tip and cluster) with voltage is proportional to the sum of the ratios of the partitioned areas to the contact areas multiplied by their normalized ''differential conductivities.'' Therefore, observed height variations in the STM image with voltage are directly proportional to the ratio of the areas of different SBH. Fitting the data in Fig. 7 (dashed lines) to the equation for the geometric dependence of the apparent height change, $\delta=2.65$ and 1.67 nm for voltage changes of 3.0 and 2.0 V, respectively. The fact that the magnitude of the edge effect, as indicated by the size of δ, increases with voltage change is consistent with an increase in band bending in the substrate. The relative values of differential conductivities also indicate that the edge effect is larger at the larger voltage; i.e., $G'_{\text{ring}}/G_{\text{eff}}$ is 0.02 at 2.0 V and 0.27 at 3 V while $G'_{\text{center}}/G_{\text{eff}}$ is 0.82 at 2.0 V and 2.45 at 3.0 V (3% at 2 V but over 10% at 3 V). At the limit of large cluster sizes the apparent height change becomes independent of cluster size at the value associated with $G'_{\text{center}}/G_{\text{center}}A_{\text{total}}$. The implicit assumption that $\delta\neq f(r)$ implies that the model may break down at very small cluster sizes and, in fact, the function diverges as $R\rightarrow 0$. While it might be tempting to consider the physical implications of the function minimum, it occurs at length scales sufficiently small (<3 or 5 nm) to question the validity of its application in that range.

In order to examine the voltage dependence in more detail, simple relations for current are put into Eq. (5). If transport through the depletion region (i.e., across the metal-semiconductor interface) can be expressed as thermionic conduction,

$$J=A^*T^2\exp[q\Phi_{\text{ring}}/kT]\exp[qV_1/kT] \tag{8}$$

then (in the forward-bias condition):

$$\begin{aligned}dW/dV=&(1/1.025\phi^{1/2})\{(q/kT)-1/V\}\exp[q(\Phi_{\text{eff}}-\Phi_{\text{center}})/kT]+(2\delta/R)(\{(q/kT)(1-\Phi'_{\text{ring}})-1/V\}\\&\times\exp[q(\Phi_{\text{eff}}-\Phi_{\text{ring}})/kT]-\{(q/kT)-1/V\}\exp[q(\Phi_{\text{eff}}-\Phi_{\text{center}})/kT])+(\delta^2/R^2)\\&\times(\{(q/kT)-1/V\}\exp[q(\Phi_{\text{eff}}-\Phi_{\text{center}})/kT]-\{(q/kT)(1-\Phi'_{\text{ring}})-1/V\}\exp[q(\Phi_{\text{eff}}-\Phi_{\text{ring}})/kT])\end{aligned} \tag{9}$$

where the Schottky barrier at the edge (Φ_{ring}) and the effective (average) Schottky barrier for the system (Φ_{eff}) are considered to be functions of voltage. It is likely that changes in the SBH of the ring are algebraic in functional form. Thus, as the applied voltage gets large, the exponents of this equation will dominate. At lower voltage, where Φ_{ring} can be considered nearly constant (or very weakly dependent on V), the terms with the prefactor $\{[q/kT(1\text{-}\Phi'_{\text{ring}})]-1/V\}$ will have a positive exponent and the terms with $\{(q/kT)-1/V\}$ will have negative exponents. Further, at lower voltages $\Phi_{\text{eff}}-\Phi_{\text{center}}$ should be small; however, $\Phi_{\text{eff}}-\Phi_{\text{ring}}$ should be nearly Φ_{center} due to the increase field density at the cluster edge. This point is also clear from the decreasing value of δ at lower voltages. Therefore, the terms with a positive exponent will dominate the functional behavior of the system at low voltages. The voltage dependence of the apparent height change, shown in Fig. 6, is a monotonically increasing-function of V. If Φ_{ring} is a linear function of V then $dW/dV\sim(C1/V)\exp[C_2V]$ where the C's are constants. This equation is shown with the data in Fig. 6 to show that it represents a reasonable description of the voltage dependence.

CONCLUSIONS

Voltage-dependent contrast in STM images has been used to quantify local barrier formation at nanoscale metal-oxide interfaces which have been described in terms of classical Schottky-barrier formation. The electronic characteristics of nanometer-sized contacts under effective-forward- and

reverse-bias conditions are mediated by the effects of finite size in these systems. The reduction of the measured contact potential relative to that of an infinite plane can be directly related to the contributions of current flow through the edges of the nanostructure. For larger clusters these edge effects are proportionally smaller. A simple geometrical model which considers the ratios of areas and effective differential-conductivities captures trends observed in height variations as a function of cluster size. Contact-potential formation in systems of this size scale with adjacent depletion zones has implications to substrate-mediated cluster-cluster interactions, surface wetting, and homogeneity in device fabrication.

ACKNOWLEDGMENTS

The authors would like to thank Professor J. DiNardo and Dr. G. Hörz for discussion and the technical staff of the Max-Planck-Institut für Metallforschung in Stuttgart for their assistance in the preparation of this work. Support through the National Science Foundation, Grant No. DMR 90-58557, the MRI program Grant No. DMR 91-20668, and by the Max-Planck-Gesellschaft is gratefully acknowledged.

[1] J. P. Sullivan, R. T. Tung, M. Pinto, and W. Graham, J. Appl. Phys. **70**, 7403 (1991).
[2] J. P. Sullivan, Ph.D. thesis, University of Pennsylvania, 1989.
[3] R. T. Tung, Appl. Phys. Lett. **58**, 465 (1984).
[4] R. T. Tung, Phys. Rev. B **45**, 13 509 (1992).
[5] R. T. Tung, *Contacts to Semiconductors* (Noyes Publications, New York, 1993), pp. 167–291.
[6] H. Palm, M. Arbes, and M. Schulz, Phys. Rev. Lett. **71**, 2224 (1993).
[7] M. H. Hecht, L. D. Bell, W. J. Kaiser, and F. J. Grunthaner, Appl. Phys. Lett. **55**, 780 (1989).
[8] M. D. Stiles and D. R. Hamann, Phys. Rev. Lett. **66**, 3179 (1991).
[9] P. J. Møller and M.-C. Wu, Surf. Sci. **224**, 265 (1989).
[10] P. J. Møller and M.-C. Wu, Surf. Sci. **224**, 250 (1989).
[11] U. Diebold, J.-M. Pan, and T. E. Madey, Phys. Rev. B **47**, 3868 (1993).
[12] P. Thibado, Ph.D. thesis, University of Pennsylvania, 1995.
[13] P. Thibado and D. A. Bonnell (unpublished).
[14] D. Novak (private cummunication).
[15] G. S. Rohrer, V. E. Henrich, and D. A. Bonnell, Surf. Sci. **278**, 146 (1992).
[16] A. Szabo and T. Engel, Surf. Sci. **329**, 241 (1995).
[17] P. W. Murray, N. G. Condon, and G. Thorton, Phys. Rev. B **51**, 10 989 (1995).
[18] A. Szabo and T. Engle, Surf. Sci. **329**, 241 (1995).
[19] Y. Liang, D. L. Carroll, and D. A. Bonnell, in *Interface Control of Electrical, Chemical, and Mechanical Properties*, edited by S. P. Murarka, K. Rose, T. Ohmi, and T. Seidel, MRS Symposium Proceedings No. 318 (Materials Research Society, Pittsburgh, 1994), p. 653.
[20] *Scanning Tunneling Microscopy and Spectroscopy*, edited by D. A. Bonnell (VCH, New York, 1993).
[21] K. Besocke, B. Krahl-Urban, and H. Wagner, Surf. Sci. **68**, 39 (1977).
[22] V. E. Henrich, G. Dresselhaus, and H. J. Zeiger, Phys. Rev. Lett. **36**, 1335 (1976).
[23] J. F. Janek, A. R. Williams, and V. L. Moruzzi, Phys. Rev. B **11**, 1522 (1975).
[24] E. Stoll, A. Baratoff, A. Selloni, and P. Carnevali, J. Phys. C **17**, 3073 (1984).
[25] W. Schottky, Z. Phys. **113**, 367 (1939).
[26] H. K. Henisch, *Semiconductor Contacts* (Oxford University Press, New York, 1984).
[27] S. M. Sze, *Physics of Semiconductor Devices* (Wiley, New York, 1990).
[28] See, for example, J. D. Jackson, *Classical Electrodynamics* (Wiley, New York, 1975).
[29] J. P. Sullivan, Ph.D. thesis, University of Pennsylvania, 1991.